Ecological Engineering 155 (2020) 105942

Contents lists available at ScienceDirect

Ecological Engineering

journal homepage: www.elsevier.com/locate/ecoleng

Flow uniformity metrics for quantifying the hydraulic and treatment performance of constructed wetlands

Shang-Shu Shih[a,b,*], Hung-Chih Wang[a]

[a] Department of Civil Engineering, National Taiwan University, Taiwan
[b] Hydrotech Research Institute, National Taiwan University, Taiwan

ARTICLE INFO

Keywords:
Constructed wetlands
Flow velocity
Advective transport
Dead zone
Short-circuiting flow
Hydraulic performance

ABSTRACT

The treatment efficiency of constructed wetlands is strongly related to hydraulic conditions. The occurrences of a dead zone and short-circuiting flow decrease flow uniformity and might decrease hydraulic performance. This study aims to investigate the relationship between spatial flow characteristics and wetland treatment performance. A hydrodynamic and contaminant transport model conducted ten sets of simulations with different water depths and five sets of simulations with varying numbers of emergent obstructions. Each experiment had a variant number, dimension, and allocation of obstructions. A metric of flow uniformity was proposed and discussed. We demonstrated how the dead zone and short-circuiting alter flow conditions and affect the hydraulic performance and pollutant treatment efficiency by examining the flow characteristics. The order-of-magnitude of time scales between the advective transport rate and diffusive transport rate was analyzed by calculating the Peclet number. The first-order model was used to calculate the pollutant removal ratio. The results revealed that the values of advection were approximately tens to hundreds of times those of diffusion, indicating that the flow velocity dominated the dispersion behavior. The significant improvement in flow uniformity was found when emergent obstructions were installed. The index value of the dead zone was 2 to 69 times that of the short-circuiting flow, which shows that the dead zone significantly affected the uniformity of the flow. In addition, we discovered that when the coverage ratio of the dead zone was less than 50%, the hydraulic efficiency increased from 0.55 to 1.00. Nevertheless, the short-circuiting flow was found to have minor effects on the hydraulic efficiency. The new methodology for distinguishing dead zones and short-circuiting flow areas is useful for evaluating hydraulic performance directly instead of executing water quality modeling or tracer experiments.

1. Introduction

Free-water surface constructed wetlands (FWSs) are beneficial not only for the reduction in particulates through sedimentation (Kadlec et al., 2010) and the removal of organic contaminants through biodegradation (Hsu et al., 2011) but also for biodiversity conservation by providing habitats for plants and animals (Zedler and Kercher, 2005). Degradation by microorganisms and adsorption by plants are the primary mechanisms for pollutant removal and degradation (Toet et al., 2005; Vymazal, 2014). The overall effectiveness of both mechanisms is dependent on the residence time, which represents how long the water and pollutants are retained in the wetland (Thackston et al., 1987; Persson et al., 1999; Su et al., 2009). The treatment efficiency of FWSs cannot be determined without understanding the flow dynamics of individual parcels of water through the wetland (Arega, 2013). Unsatisfactory hydraulic control is one of the causal factors in the poor performance of FWSs as water pollution control facilities (Reed et al., 1995). Many studies have indicated that short-circuiting flow, flow circulation, and dead zones may reduce the treatment efficiency of wetlands (Holland et al., 2004; Dierberg et al., 2005; Bracho et al., 2006). Chang et al. (2016) indicated that these synthetic effects may appear as low flow uniformity and hydraulic efficiency. Wetlands with emergent obstructions and submerged obstructions with vegetation are significantly more efficient than non-vegetated wetlands at increasing hydraulic performance (Shih et al., 2016) and removing pollutants (Musner et al., 2014). Recent numerical studies have investigated the efficiency of idealized wetlands as a function of vegetation distribution and wetland shape (Sabokrouhiyeh et al., 2017; Savickis et al., 2016). The results indicated that the density and extent of the obstructions and heterogeneous vegetation were positively correlated with hydraulic efficiency by reducing the area of dead zones at the wetland corners (Chang et al., 2016; Sabokrouhiyeh et al., 2020).

* Corresponding author at: No. 1, Sec.4, Roosevelt Rd., 106 Taipei City, Taiwan.
E-mail address: uptreeshih@ntu.edu.tw (S.-S. Shih).

https://doi.org/10.1016/j.ecoleng.2020.105942
Received 26 February 2020; Received in revised form 2 June 2020; Accepted 10 June 2020

The treatment potential and efficiency of wetlands are usually related to the residence time of each individual fluid particle of pollutants within the wetland (Su et al., 2009; Wahl et al., 2010). Numerical studies which have investigated the efficiency of idealized wetlands as a function of vegetation distribution and wetland shape. The travel of fluid particles in an FWS consists of two phenomena in conservative water quality modeling, including advective and dispersive effects (Fischer et al., 1979). The traditional method in the past for obtaining hydraulic performance is through water quality modeling combined with hydrodynamic modeling to calculate the hydraulic retention time. We hypothesize that advection effects are dominant rather than dispersion effects on treatment efficiency, and the area of the dead zone (slow-flow velocity area) and short-circuiting flow (high-flow velocity area) would decrease the flow uniformity and hydraulic performance. The primary purpose of this study is to distinguish the low-velocity regions and the high-flow areas from the flow field calculated by a hydrodynamic model. From calculating the steps of the pollutant and tracer transport mode, the hydraulic performance of the wetland can be understood directly by investigating the variant characteristics of variant flow fields. The objective of the study is to provide flow uniformity metrics to separate these two areas from others and thus may replace the traditional methods and metrics for evaluating hydraulic performance. A reliable horizontal two-dimensional model is employed to simulate the flow conditions and tracer concentrations from fifty hypothetical cases.

2. Materials and methods

2.1. Hypothetic cases

The FWS was designed as 75 m long and 40 m wide, giving it an aspect ratio of 1.88 (wetland length over wetland width). The inlet and outlet are located at the upper-right corner and the lower-left corner of the wetland, respectively, as shown in Fig. 1a. The upstream boundary condition was set as the inflow discharge of 0.04 $m^3 s^{-1}$ in RMA2 and the inflow concentration of 10 mg L^{-1} in RMA4. The downstream boundary condition, the outlet water surface elevation, was set according to the different scenarios as discussed later. To evaluate the improvement in the hydraulic efficiency under treatments with different modifications, the empty FWS is conducted as the reference case. This empty wetland has the layout mentioned above and no obstructions. The model parameters were set as suggested by Chang et al. (2016).

There are fifty conditions for evaluation, including five sets of simulations with different numbers of emergent obstructions (EOs) and ten games of simulations with varying depths of water, respectively. EOs were utilized as a kind of flow barriers to change the flow conditions of FWSs with the designation of 30 m long and 1 m wide. They were evenly spaced within the wetland, and their number ranged from one to four, as shown in Fig. 1a. The numerical grids were removed from the locations at which the EOs were placed, representing a rigid boundary around the EOs and no flux exchange through the EOs. They may mainly be concerning cases that need improved flow uniformity and hydraulic performance. Moreover, Holland et al. (2004) and Shih et al. (2013) found that increasing the water depth elicits a decrease in hydraulic efficiency. For practical purposes, the USEPA (2000) suggested the use of integrated FWSs with both shallow- and deep-water FWSs to enable various biochemical reactions occurring under aerobic and anaerobic conditions. In the present study, both shallow-water and deep-water FWSs were investigated and analyzed. The simulated water depths varied from 0.7 m to 2.5 m, with an incremental increase in depth of 0.2 m, as shown in Fig. 1b. Water depths greater than 1.2 m were classified as deep-water cases.

2.2. Hydrodynamic model

RMA2 is a two-dimensional depth-averaged finite element hydrodynamic model for computing the water surface elevations and horizontal velocity components of the subcritical free-surface flow field (Donnell et al., 2009). The governing equations of RMA2 pertain to mass and momentum conservation, ignoring the effects of earth's angular rotation and wind shear, as shown in Eqs. (1), (2), and (3). There are 3002 to 3418 numerical grids in different cases with different numbers of EOs, and each grid size is 1 × 1 m^2. The EOs acted as a kind of flow barriers and were constructed as an enclosed, rigid boundary with no flux exchange.

$$\frac{\partial h}{\partial t} + \frac{\partial (hu)}{\partial x} + \frac{\partial (hv)}{\partial y} = 0 \quad (1)$$

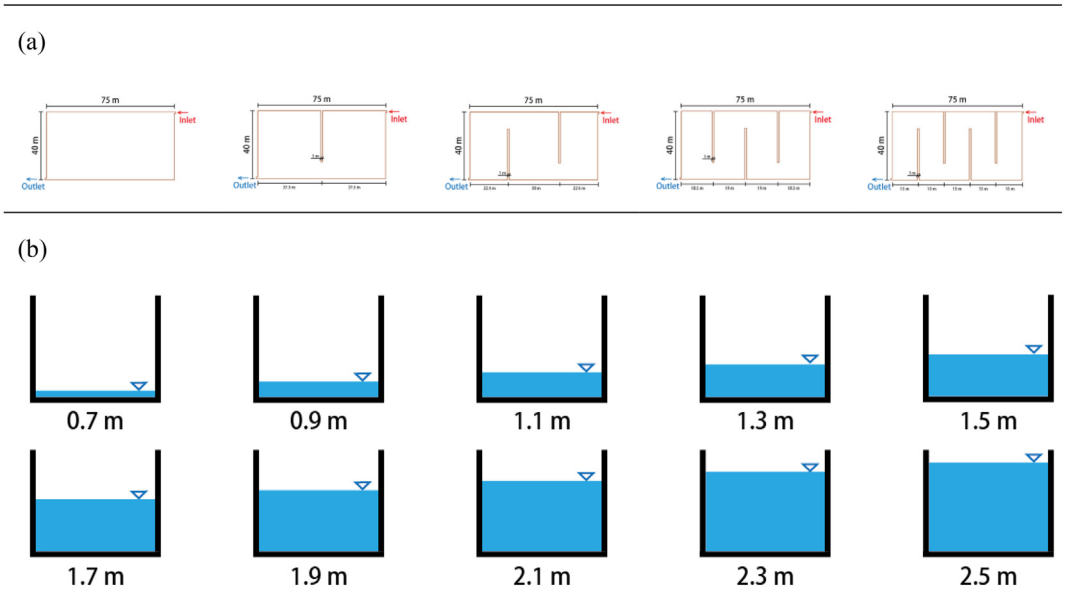

Fig. 1. Schematic plot for the numerical experiments of the fifty hypothetical cases. Each case has the same dimensions with length 75 m and width 40 m. (a) Five sets of numbers of emergent obstructions (EOs), and (b) ten water depths are investigated.

$$h\frac{\partial u}{\partial t} + hu\frac{\partial u}{\partial x} + hv\frac{\partial u}{\partial y} - \frac{1}{\rho}\left[\frac{\partial}{\partial x}\left(hE_{xx}\frac{\partial u}{\partial x}\right) + \frac{\partial}{\partial y}\left(hE_{xy}\frac{\partial u}{\partial y}\right)\right] + gh\left(\frac{\partial z_b}{\partial x} + \frac{\partial h}{\partial x}\right) + \frac{gun^2}{h^{1/6}}(u^2 + v^2)^{1/2} = 0 \quad (2)$$

$$h\frac{\partial v}{\partial t} + hu\frac{\partial v}{\partial x} + hv\frac{\partial v}{\partial y} - \frac{1}{\rho}\left[\frac{\partial}{\partial x}\left(hE_{yx}\frac{\partial v}{\partial x}\right) + \frac{\partial}{\partial y}\left(hE_{yy}\frac{\partial v}{\partial y}\right)\right] + gh\left(\frac{\partial z_b}{\partial y} + \frac{\partial h}{\partial y}\right) + \frac{gvn^2}{h^{1/6}}(u^2 + v^2)^{1/2} = 0 \quad (3)$$

where x and y are the Cartesian coordinates of the horizontal and longitudinal directions, respectively, in [m]; t is time in [s]; ρ is the water density in [kg m^{-3}]; h is the water depth in [m]; u and v are the velocities in the x- and y-directions, respectively, in [m s^{-1}]; z_b is the elevation of the bottom in [m]; E_{xx}, E_{yy}, E_{xy}, and E_{yx} are the eddy viscosities, in [Pascal s], representing the molecular viscosity and the effects of turbulence from Reynold's stress terms in the governing equations, and was set as 20 by the suggestion of Donnell et al. (2009); n is the roughness coefficient of Manning's formula, in [$m^{-1/3}$ s]. The Manning's n of the wetland bed was set as 0.035 based on Woody's roughness coefficient table (Cowan, 1956).

2.3. Contaminant transport model

The node, grid, water depth, and flow velocity are developed and calculated by the RMA2 model and input as given values for executing the contaminant transport model, RMA4. RMA4 is a depth-averaged water quality transport model in which the depth concentration distribution is assumed to be uniform (Letter and Donnell, 2008) and was used for simulating the pulse tracer experiments. The governing equation of RMA4 is the advection and dispersion equation dealing with the transport and mixing process. The source/sink of the constituent and the rainfall/evaporation rate were neglected. Since conservative simulations were considered in the study, the governing equation was simplified, as shown in Eq. (4).

$$\frac{\partial c}{\partial t} + u\frac{\partial c}{\partial x} + v\frac{\partial c}{\partial y} - \frac{1}{h}\frac{\partial}{\partial x}hD_x\frac{\partial c}{\partial x} - \frac{1}{h}\frac{\partial}{\partial y}hD_y\frac{\partial c}{\partial y} = 0 \quad (4)$$

where c is the tracer concentration in [μg L^{-1}]; h is the water depth, in [m]; u and v are the flow velocity, in [m s-1]; D_x and D_y are the diffusion coefficients in [m^2 s^{-1}]. According to the suggestion of Letter and Donnell (2008) and Chang et al. (2016) for considering the shallow water and slow flow in wetlands, the diffusion coefficients, D, was set as 0.0008 m^2 s^{-1}.

2.4. Retention time and hydraulic performance metrics

To assess the treatment efficiency and hydraulic performance of the wetlands, Persson et al. (1999) presented a hydraulic efficiency equation (Eq. (5)):

$$\lambda = e_v\left(1 - \frac{1}{N}\right) \quad (5)$$

where e_v is the effective volume ratio and N is the number of continuously stirred tank reactors in series. The hydraulic efficiency can be categorized into three levels: (Arega, 2013) good hydraulic efficiency, $\lambda \geq 0.75$; (Bracho et al., 2006) satisfactory hydraulic efficiency, $0.5 < \lambda < 0.75$; and (Chang et al., 2016) poor hydraulic efficiency, $\lambda \leq 0.5$.

According to Thackston et al. (1987), e_v indicates the utilization of the effective volume ratio of a detention system, according to Eq. (6):

$$e_v = \frac{t_m}{t_n} \quad (6)$$

where t_n is the mean residence time in [hr], as shown in Eq. (7), and t_m is the nominal retention time in [hr]:

$$t_n = \frac{V}{Q} \quad (7)$$

where V is the volume of the pond in [m^3], and Q is the flow rate in [m^3 s^{-1}]. The t_m can be calculated from the first moment of the response curve, as shown in Eq. (8):

$$t_m = \frac{\int_0^\infty tcdt}{\int_0^\infty cdt} \approx \frac{\sum_{i=2}^{n}\left(\frac{t_i c(t_i) + t_{i-1}c(t_{i-1})}{2}\right)(t_i - t_{i-1})}{\sum_{i=2}^{n}\left(\frac{c(t_i) + c(t_{i-1})}{2}\right)(t_i - t_{i-1})} \quad (8)$$

where c is the tracer concentration in [μg L^{-1}], t is the time of measurement in [hr], and n represents the last survey of the recorded concentration and time.

Kadlec and Knight (1996) suggested an alternative formula for calculating N based on differences in the time of the peak outflow concentration and the nominal retention time (Eq. (9)):

$$N = \frac{t_n}{t_n - t_p} \quad (9)$$

where t_p is the time of the peak concentration in the tracer response curve measured at the outlet of the pond in [hr].

Chang et al. (2016) substituted Eqs. (6) and (9) into Eq. (5) to obtain the hydraulic efficiency formula (Eq. (10)), which is used to estimate the hydraulic efficiency in the present study.

$$\lambda = \frac{t_m \times t_p}{t_n^2} \quad (10)$$

2.5. Pollutant treatment efficiency

The first-order model was applied for calculating pollutant removal, as shown in Eq. 11. The model considers physical, microbial, and biochemical processes for treating wastewater. A number of studies have indicated different values of the decay constant k_t for local purposes (USEPA, 1988; Hammer, 1989; Cooper et al., 1996). In this study, k_t was set as 0.3 day^{-1} by the suggestion of Shih et al. (2013).

$$R = 1 - \frac{C_e}{C_i} = 1 - e^{-k_t t_m} \quad (11)$$

Where R represents pollutant removal ratio, C_i and C_e represent influent and effluent concentrations in [mg L^{-1}], k_t represents the decay constant in [day^{-1}], and t_m is the nominal retention time in [hr].

2.6. Flow uniformity metric

The flow uniformity metric is proposed by this study for quantifying the uniformity of a flow velocity field in a constructed wetland. The flow uniformity metric (Φ) consists of two sub-indices, which are dead-zone ratio (DZ) and a short-circuiting flow ratio (SC), as described in Eqs. (12), (13), and (14). The Φ, DZ and SC range from 0 to 1. The summation of DZ and SC is smaller than 1. The larger the value of Φ, the more uniform the flow, and the hydraulic performance and treatment efficiency are supposed to be more significant.

$$\Phi = 1 - (DZ + SC) \quad (12)$$

$$DZ = \frac{A_{dead-zone}}{A_{total}} \quad (13)$$

$$SC = \frac{A_{short-circuiting}}{A_{total}} \quad (14)$$

where DZ, SC, and Φ represent the coverage ratio of the dead zone and short-circuiting flow and the combined effects of flow uniformity, respectively, ranging from 0 to 1; and A_{total}, $A_{dead\text{-}zone}$, and $A_{short\text{-}circuiting}$ represent the coverage areas of the whole area, dead-zone area, and

short-circuiting area of wetlands.

3. Results and discussion

3.1. Dominant advection effects

Contaminant transportation is described as the combined effects of advection, dispersion, and reaction, as shown in Eq. (4). The advection term represents the effects of flow velocity, while the dispersion term represents those of diffusion and shear flow dispersion (Fischer et al., 1979). The reaction effect represents the nonconserved term induced by physical and biochemical processes and is influenced by the residence time in constructed wetlands (Shih et al., 2013). Since conservative simulations were considered in this study, the reaction term was neglected. The order-of-magnitude methods were sometimes used in a mixing problem to obtain a very preliminary solution and are dependent on the most critical parameters. Such analyses are based on dimensional analysis, with some coefficients investigated from experiments or the previous solutions of differential equations (Fischer et al., 1979). The analysis of the order-of-magnitude was used to determine the dominant effects of contaminant transportation. The order-of-magnitude analyses in calculating the values of the advection term and dispersion term simulated by the hydrodynamic and contaminant transport models were obtained in the present study. The values of the advection and dispersion terms were expressed as time scales and obtained by calculating the grid size divided by the flow velocity and the square of the grid size divided by the dispersion coefficient. The ratio between the advective transport rate and the dispersive transport rate can also be determined by the well-known dimensionless parameter Peclet number (Persson and Wittgren, 2003). The values of the Peclet number indicate the advective transport rates of the fifty cases were tens to hundreds of times those of the dispersive transport rates, as shown in Table 1. The advection effect was discovered to be much more significant than the dispersion effect in the present study; this outcome is supportive of previous studies (Fischer, 1967; Persson and Wittgren, 2003). We thus focus on determining the spatial distribution of flow velocity representing advection effects in the variant cases to understand the relationship among flow patterns and hydraulic performance and treatment efficiency. The influences of the separated dead zone and short-circuiting flow and combined effects were also calculated and discussed.

We investigated the velocity dynamics at each node in the wetland by altering the location and number of EOs to reduce the area of the dead zone. The hydrodynamic model calculated the flow velocity of each node, and an interval of 1×10^{-3} m s^{-1} discretized the values. The velocity probability distribution of the frequency of occurrence in fifty cases is presented in Fig. 2. The results showed that the pattern of the velocity probability distribution is significantly related to the water depth and the number of EOs. In the case of no EOs and one EO, the velocity probability distribution revealed a right-skewed distribution, and the deeper the water depth was, the more obvious the right-skewed phenomenon. In the case of two or more EOs, the probability distribution of flow velocity was close to the normal distribution, and the proportion of low-flow areas decreased with the increase in the number of EOs. The impact on deep-water wetlands was found to be higher than that on shallow wetlands. Moreover, the increase in water depth slows down the average flow velocity, and the associated low-flow velocity regions are more affected, possibly resulting in a decrease in hydraulic efficiency.

3.2. Identification of dead zone and short-circuiting

In constructed wetlands, the dead zone area and short-circuiting flow are the critical causes that affect residence time, hydraulic performance and treatment efficiency (Su et al., 2009; Shih et al., 2017). The study examined several thresholds to define dead zone areas and short-circuiting flow for calculating the coverage ratio of these two areas and the related Φ as the following three steps: (Arega, 2013) normalize the low-velocity areas with different thresholds divided by 1×10^{-3} m s^{-1}, and then draw the relationship between the area ratio of the low-velocity areas and the hydraulic efficiency; (Bracho et al., 2006) normalize the high-velocity areas with different thresholds divided by average velocity, and then draw the relationship between the area ratio of the high-velocity region and the hydraulic efficiency; (Chang et al., 2016) calculate the correlation between different thresholds and hydraulic efficiency and determine the thresholds with the highest correlation coefficient for defining the thresholds of dead zone and short-circuiting flow.

The correlation coefficient between dead zone area and hydraulic efficiency is analyzed, ranging from 0.28 to 0.77, as shown in Fig. 3a. The highest relationship is discovered around the flow velocity of 1×10^{-3} m s^{-1}. The results reveal that when the overall average flow velocity is less than 1×10^{-3} m s^{-1}, the hydraulic efficiency drops below 0.7. We therefore define the threshold of the low-velocity region at 1×10^{-3} m s^{-1} for classifying whether the areas are dead zones or not. With the dead-zone threshold, we calculate the dead-zone area in every case and then plot the hydraulic efficiency against the dead-zone area in Fig. 3b. The results show that no EOs and one EO have relatively high dead zone area ratios. When the area ratio of the flow velocity that is 1×10^{-3} m s^{-1} is greater than 50%, the hydraulic efficiency also decreases. The mean ratios of no EOs and one EO are 0.60 and 0.62, respectively, and vary with water depth. The dead zone occurs at the corner and behind the obstruction. Especially with one EO, the dead zone occurs behind the obstruction with a large area. In contrast, two and four EOs show a relatively low-velocity area ratio. Compared to the flow field graph, the dead zone is decreased mainly due to the EOs and the alignment. The dead zone only occurs at the corner, and the area is much smaller.

Short-circuiting has been recognized as one of the largest obstacles to the successful design and management of treatment wetlands (Persson, 2000). The high-velocity area ratio beyond the threshold is calculated and found to be correlated with hydraulic efficiency. Repeating the above procedure, we change the coefficient slightly until we yield the best short-circuiting flow threshold. However, the short-circuiting flow seems not to be significant (Fig. 3c). In our cases, the correlation coefficient is 0.69, and the short-circuiting flow area is relatively small ($0.01 < SC < 0.05$), as shown in Fig. 3d. The significant correlation between short-circuiting flow and mixing highlights the profound effect on hydraulic performance (Liu et al., 2020), indicating the necessity of reducing short-circuiting flow (Guzman et al., 2018). We used the moment index (MI), Morril index (Mo), and the 5% normalized time (t_5), which were presented by Wahl et al. (2010) and Farjood et al. (2015), to evaluate the hydraulic performance and the related short-circuiting. The t_5 is the normalized time for 5% of the added tracer to exit wetlands, while the Mo is defined as t_{90}/t_{10}, where t_{10} and t_{90} are the times for 10% and 90% of the added tracer to exit the system, respectively (Farjood et al., 2015). Mo^{-1} is the reciprocal of Mo. The MI for hydraulic efficiency introduced by Wahl et al. (2010). Farjood et al. (2015) suggested that MI > 0.75 and $t_5 > 0.3$ recognize good hydraulic performance. According to their suggestion, we found that our cases mostly have a t_5 index higher than 0.3, indicating that short-circuiting flow is not significant. We propose that the short-circuiting flow threshold occurs in the elbow point and reveals the value of approximately three times the mean velocity, as shown in Fig. 3e. Please refer to Farjood et al. (2015) for the code details of the variant baffle configurations. Although increasing the threshold of short-circuiting leads to a higher correlation, the high-velocity zone is decreasing dramatically. We thus choose three times the mean velocity to be the short-circuiting flow area threshold. On the other hand, short-circuiting flow mainly occurs at the inlet and outlet of the wetland and some narrow part in the one EO case. Since short-circuiting flow has a small area, it seems to have a minor effect. With the above analysis, we

Table 1
Several cases with a different number of emergent obstructions and the related flow characteristics, hydraulic performance, flow uniformity, and Peclet number.

No.	H (m)	V (X10^{-3} m s^{-1})	t_m (hr)	e_v	λ	R (%)	DZ	SC	Φ	Pe
0	0.7	2.19 ± 3.30 (1.51)	13.55	0.93	0.52	16	0.29	0.04	0.67	232
0	0.9	1.58 ± 2.51 (1.58)	16.97	0.91	0.54	19	0.39	0.04	0.57	168
0	1.1	1.24 ± 2.02 (1.63)	21.09	0.92	0.56	23	0.50	0.04	0.47	132
0	1.3	1.03 ± 1.69 (1.64)	22.87	0.84	0.43	25	0.64	0.03	0.32	110
0	1.5	0.87 ± 1.45 (1.66)	26.09	0.83	0.45	28	0.75	0.03	0.22	93
0	1.7	0.80 ± 1.28 (1.60)	31.24	0.88	0.47	32	0.81	0.03	0.16	85
0	1.9	0.70 ± 1.13 (1.61)	35.51	0.90	0.64	36	0.85	0.03	0.12	75
0	2.1	0.63 ± 1.02 (1.62)	32.41	0.74	0.38	33	0.88	0.03	0.08	67
0	2.3	0.61 ± 0.93 (1.52)	38.06	0.79	0.47	38	0.91	0.03	0.07	65
0	2.5	0.57 ± 0.85 (1.49)	40.00	0.77	0.43	39	0.92	0.02	0.06	60
1	0.7	2.30 ± 3.46 (1.50)	13.29	0.92	0.54	15	0.42	0.03	0.54	244
1	0.9	1.69 ± 2.62 (1.55)	16.64	0.90	0.55	19	0.48	0.04	0.47	179
1	1.1	1.34 ± 2.12 (1.57)	23.08	1.00	0.55	25	0.50	0.04	0.45	143
1	1.3	1.10 ± 1.76 (1.60)	25.84	0.96	0.48	28	0.58	0.04	0.38	117
1	1.5	0.98 ± 1.51 (1.55)	27.03	0.87	0.42	29	0.64	0.04	0.32	104
1	1.7	0.90 ± 1.31 (1.45)	31.16	0.89	0.42	32	0.71	0.03	0.27	96
1	1.9	0.78 ± 1.16 (1.49)	30.67	0.78	0.50	32	0.73	0.02	0.25	83
1	2.1	0.71 ± 1.07 (1.51)	35.54	0.82	0.42	36	0.78	0.03	0.19	75
1	2.3	0.70 ± 0.95 (1.36)	40.04	0.84	0.35	39	0.80	0.02	0.18	74
1	2.5	0.67 ± 0.86 (1.28)	39.62	0.77	0.45	39	0.69	0.01	0.30	94
2	0.7	3.06 ± 3.20 (1.04)	14.99	1.00	0.85	17	0.14	0.02	0.84	325
2	0.9	2.34 ± 2.41 (1.03)	19.13	1.00	0.80	21	0.17	0.01	0.81	248
2	1.1	1.92 ± 1.95 (1.01)	23.36	1.00	0.86	25	0.21	0.01	0.78	204
2	1.3	1.59 ± 1.70 (1.07)	27.47	1.00	0.78	29	0.23	0.01	0.76	185
2	1.5	1.40 ± 1.39 (1.00)	31.45	1.00	0.76	33	0.32	0.01	0.67	148
2	1.7	1.28 ± 1.26 (0.99)	35.36	1.00	0.71	36	0.37	0.01	0.62	136
2	1.9	1.12 ± 1.11 (0.99)	39.81	1.00	0.92	39	0.47	0.01	0.52	119
2	2.1	0.97 ± 0.98 (1.01)	42.88	1.00	0.69	41	0.65	0.01	0.34	103
2	2.3	0.93 ± 0.94 (1.01)	47.04	1.00	0.63	44	0.65	0.01	0.34	99
2	2.5	0.89 ± 0.86 (0.97)	50.68	0.99	0.77	47	0.69	0.01	0.30	94
3	0.7	3.21 ± 3.28 (1.02)	13.32	0.94	0.80	15	0.20	0.01	0.79	341
3	0.9	2.48 ± 2.50 (1.01)	16.79	0.92	0.81	19	0.21	0.01	0.78	263
3	1.1	2.01 ± 2.01 (1.00)	20.43	0.92	0.81	23	0.22	0.01	0.77	213
3	1.3	1.74 ± 1.70 (0.98)	24.23	0.92	0.78	26	0.23	0.01	0.76	185
3	1.5	1.49 ± 1.46 (0.98)	27.67	0.91	0.81	29	0.26	0.01	0.73	159
3	1.7	1.30 ± 1.27 (0.98)	31.10	0.91	0.79	32	0.29	0.01	0.70	138
3	1.9	1.19 ± 1.14 (0.96)	35.85	0.93	0.78	36	0.31	0.01	0.68	126
3	2.1	1.06 ± 1.04 (0.98)	38.90	0.92	0.73	39	0.39	0.01	0.60	113
3	2.3	0.96 ± 0.93 (0.97)	46.47	1.00	0.78	44	0.52	0.01	0.47	102
3	2.5	0.88 ± 0.87 (0.99)	44.71	0.88	0.72	43	0.62	0.01	0.37	94
4	0.7	4.30 ± 2.81 (0.65)	14.94	1.00	1.00	17	0.02	0.01	0.97	457
4	0.9	3.34 ± 2.13 (0.64)	18.96	1.00	1.00	21	0.03	0.01	0.97	354
4	1.1	2.73 ± 1.72 (0.63)	22.99	1.00	1.00	25	0.03	0.01	0.96	290
4	1.3	2.26 ± 1.44 (0.64)	27.01	1.00	1.00	29	0.04	0.01	0.95	241
4	1.5	2.00 ± 1.25 (0.63)	31.02	1.00	1.00	32	0.05	0.01	0.94	212
4	1.7	1.74 ± 1.10 (0.63)	35.04	1.00	1.00	35	0.08	0.01	0.91	185
4	1.9	1.62 ± 1.00 (0.62)	39.05	1.00	0.99	39	0.08	0.01	0.91	172
4	2.1	1.43 ± 0.89 (0.62)	42.92	1.00	0.93	42	0.12	0.01	0.88	152
4	2.3	1.32 ± 0.84 (0.63)	47.09	1.00	0.97	44	0.16	0.01	0.84	140
4	2.5	1.23 ± 0.75 (0.61)	51.10	1.00	0.92	47	0.17	0.01	0.82	131

Note: The values of flow velocity are shown as the mean ± standard deviation, and the values in parentheses represent the coefficient of variation.

know that both the dead-zone area and short-circuiting flow zone contribute to poor hydraulic performance and treatment efficiency, and this contribution confirms the hypothesis of this study. Although the critical cause of poor treatment efficiency is the dead zone area in the present study, it could be short-circuiting flow and even circulation zone in other cases.

3.3. Hydraulic performance and treatment efficiency

The mean velocity ranges from 0.43 × 10^{-3} ms^{-1} to 4.31 × 10^{-3} ms^{-1} (Table 1). The greatest and smallest flow velocities were discovered in cases 41 (four EOs; water depth 0.7 m) and 10 (no EOs; water depth 2.5 m), respectively. Higher coefficients of variation (CV) were found in deep-water cases than in shallow-water cases, suggesting that the increase in water depth would produce a more non-uniform flow field. Generally, the greater the number of EOs installed, the higher the CVs obtained, revealing that EO significantly helps produce a more uniform flow velocity field. The addition of EOs induced longer flow pathways and less low-flow velocity area, indicating a better hydraulic performance and higher residence time. For each case, the nominal retention time increase when the water depth increases. The difference occurs at the peak concentration time. When the obstructions increase, the peak concentration time was delayed. The results suggest that the water stays in a constructed wetland for a longer time and would result in better hydraulic efficiency.

In addition, increased low-flow velocity areas are discovered when the water depth is increased to decrease the flow uniformity and hydraulic performance, as shown in Fig. 4a, b. For the no EOs cases, the hydraulic efficiency ranges from 0.38 to 0.64, indicating poor to satisfactory hydraulic performance. This result reveals that the flow path and velocity filed are not affected by the obstructions and are prone to short-circuiting flow or dead zone, so the hydraulic performance is generally poor. With one EO, the obstruction lies in the middle of the site. Nevertheless, it seems that the disturbance to the water flow is not strong enough, and the hydraulic efficiency is close to that with no obstruction. In contrast, two and three EOs yield better hydraulic

Fig. 2. The probability distribution of flow velocity expressed by the frequency of each interval of flow velocity. The red line indicates the low-velocity zone and represents the dead zone. (For interpretation of the references to colour in this figure legend, the reader is referred to the web version of this article.)

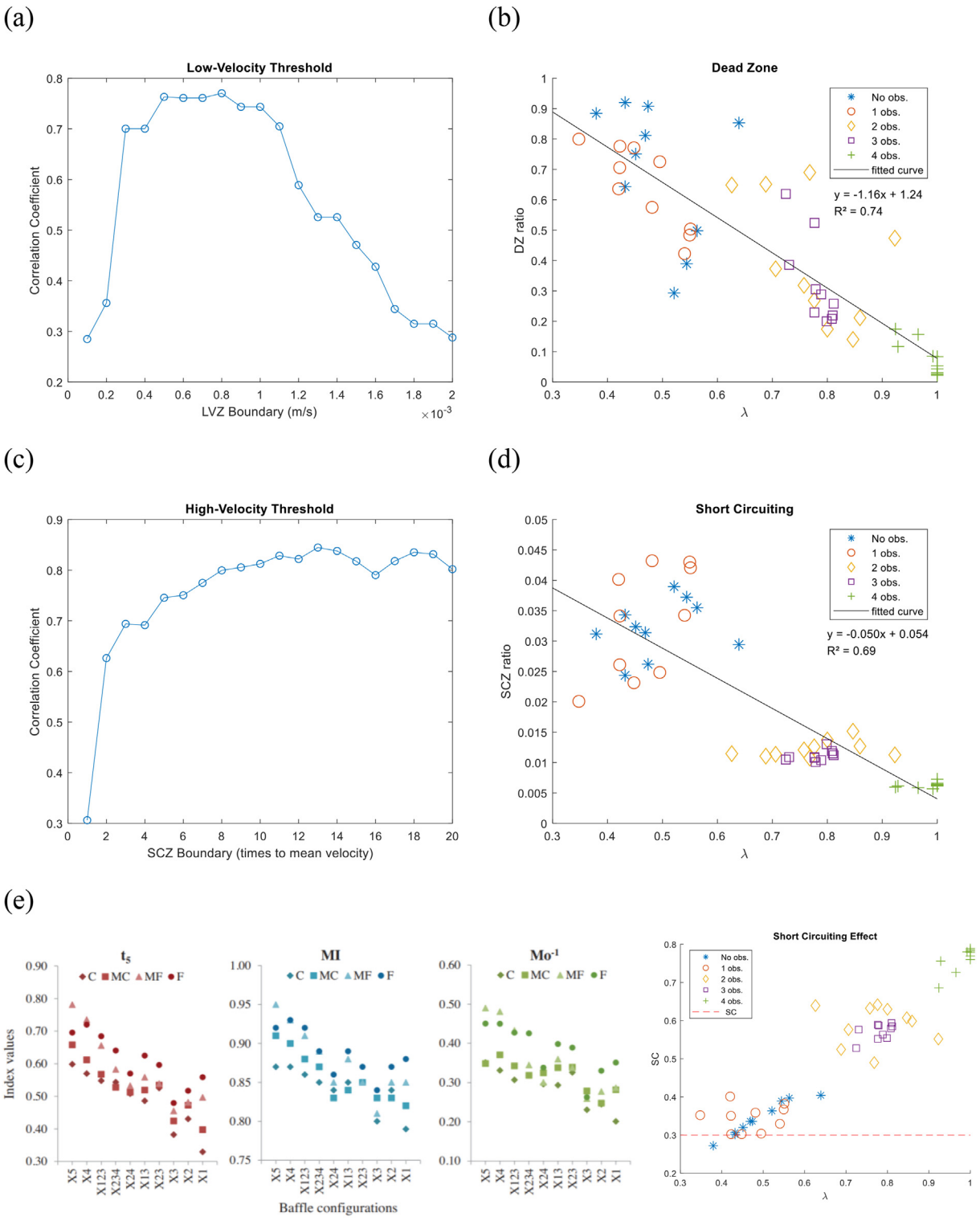

Fig. 3. Investigation of the velocity thresholds for determining the dead zone and short-circuiting flow. (a) The correlation between the low-velocity boundary and related hydraulic efficiency. The red circle indicates the threshold of the dead zone. (b) A linear negative relationship between hydraulic efficiency and the coverage ratio of the dead zone. (c) The correlation between the high-velocity boundary and related hydraulic efficiency. The red circle indicates the threshold of short-circuiting flow. (d) A linear negative relationship between hydraulic efficiency and the coverage ratio of short-circuiting. (e) The comparison of the SC value and hydraulic efficiency, indicating a minor effect of short-circuiting on affecting the hydraulic performance. (For interpretation of the references to colour in this figure legend, the reader is referred to the web version of this article.)

efficiency. The flow becomes meandering in the site and takes a longer time until it flows out, leading to better efficiency. Cases with four obstructions are the best obstruction alignment, in which the flow meanders the most and yields the best hydraulic and treatment efficiencies (Table 1). The reason why the hydraulic efficiency is not high is that dead zones are prone to occur in wetlands without obstructions. The flow velocity in these places is slow, and circulation may occur, so pollutants may be trapped here for a long time and then

(a)

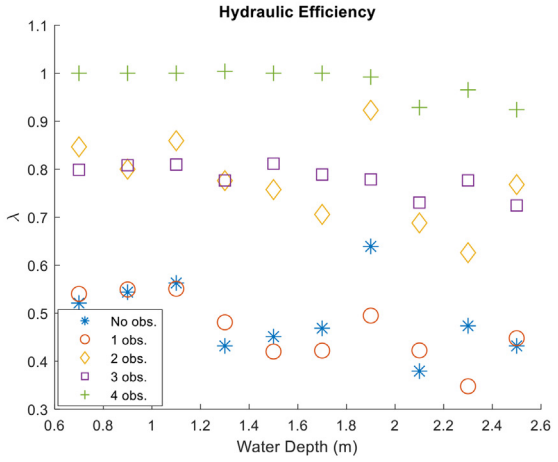

(b)

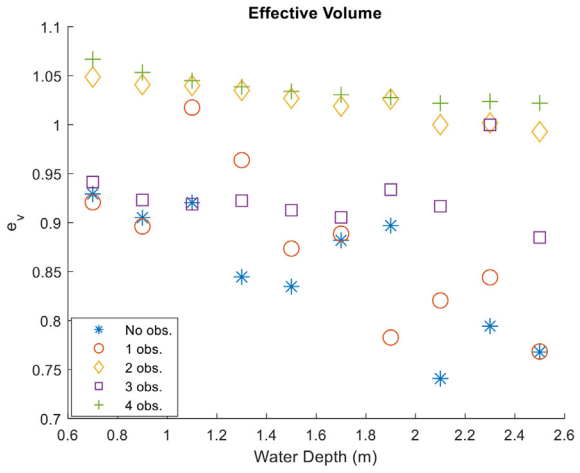

(c)

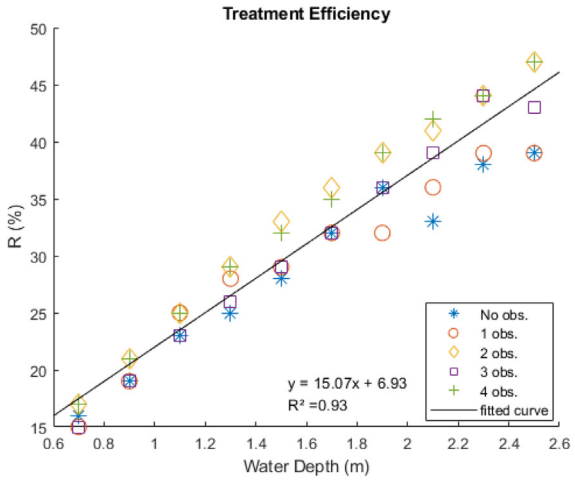

Fig. 4. The hydraulic performance and treatment efficiency in different cases, including (a) hydraulic efficiencies, (b) effective volume ratio, and (c) removal ratio with several sets of water depths and the number of emergent obstructions.

slowly dissipate. Treatment efficiency (R) was found to be positively proportional to nominal retention time and negatively correlated in increasing water depths. The more the number of the EOs, the higher the nominal retention time and the related treatment efficiency. However, the treatment efficiency (R), ranging from 15% to 47%, is not sensitive similar to the hydraulic efficiency (λ), ranging from 0.35 to 1.00, when the flow uniformity (Φ) is altered from 0.06 to 0.97, as shown in Fig. 4c. Increasing the homogenization of the flow field increases the hydraulic retention time from 13 to 51 h; nevertheless, the treatment efficiency performs poor to satisfactory. This phenomenon indicates that the hydraulic retention time still needs to be extended to optimizing the treatment performance. Several studies proved that planting emergent vegetation is useful to improve treatment performance in constructed wetlands (Musner et al., 2014; Shih et al., 2016; Sabokrouhiyeh et al., 2020).

3.4. Flow uniformity and hydraulic performance

The spatial flow velocity of the fifty cases is shown in Fig. 5. The red area in the figure represents the dead zone, which means flow velocity lower than 1×10^{-3} ms^{-1}. The blue area represents the short-circuiting zone and shows the flow velocity larger than three times the mean velocity. Otherwise, the green region represents the flow velocity between the dead zone and the short-circuiting zone, which is determined as a good performance area. The results showed that the dead zone increases with increasing water depth. The dead zone has a dramatic drop with two and four obstructions, which alter the water flow, and it becomes more meandering. The meandering channel formed by the emergent obstructions not only delays the peak arrival time and reduces the short-circuiting areas but also increases the aspect ratio and creates a longer flow path (Chang et al., 2016). In contrast, one and three EOs still have a large ratio of dead zone behind the obstructions. Preferential flow is defined as a flow that is relatively faster and causes short-circuiting (Persson et al., 1999; Su et al., 2009; Savickis et al., 2016). The simulation of EOs mainly reduced flow circulation formation and avoided few short-circuiting flows, thereby maintaining flow uniformity.

The value of SC ranges from 0.01 to 0.04 and contributes 1% to 5% to decreasing flow uniformity, while the DZ ranges from 0.02 to 0.92 and contributes 67% to 99% to that. The dead zone plays a major role in decreased flow uniformity and hydraulic performance in the present study. Obstructions were installed to improve the hydraulic performance of a deep-water constructed wetland based on the suggestions of previous studies (Nighman and Harbor, 1997; Su et al., 2009; De Oliveira et al., 2011; Chang et al., 2016). A large ratio of dead zone remained in the cases without installing EOs and with one and three EOs. After the flow passes the obstruction, it separates from the main flow and circulates or stops at the corner or behind the obstructions. Two and four EOs were found to be better than other cases because they alter the water flow, and the area behind the obstructions is smaller. Chang et al. (2016) suggested that installing obstructions on the same side of the inlet and outlet is useful for avoiding flow circulation. We discovered similar results that two and four EOs were satisfied with this principle, but one and three EOs were not. This is due to the separation of flow and water circulating or stopping at this location. The water flows uniformly in those cases and thus yields better hydraulic performance.

The values of Φ range from 0.06 to 0.97 with the corresponding hydraulic efficiency ranging from 0.43 to 1.00 and the effective ratio ranging from 0.77 to 1.00. High correlations are discovered between the flow uniformity and hydraulic performance, as shown in Fig. 6 and Eqs. (15) and (16).

$$\Phi = 1.21\lambda - 0.29;\ R^2 = 0.77 \tag{15}$$

$$\Phi = 2.47e_v - 1.78;\ R^2 = 0.60 \tag{16}$$

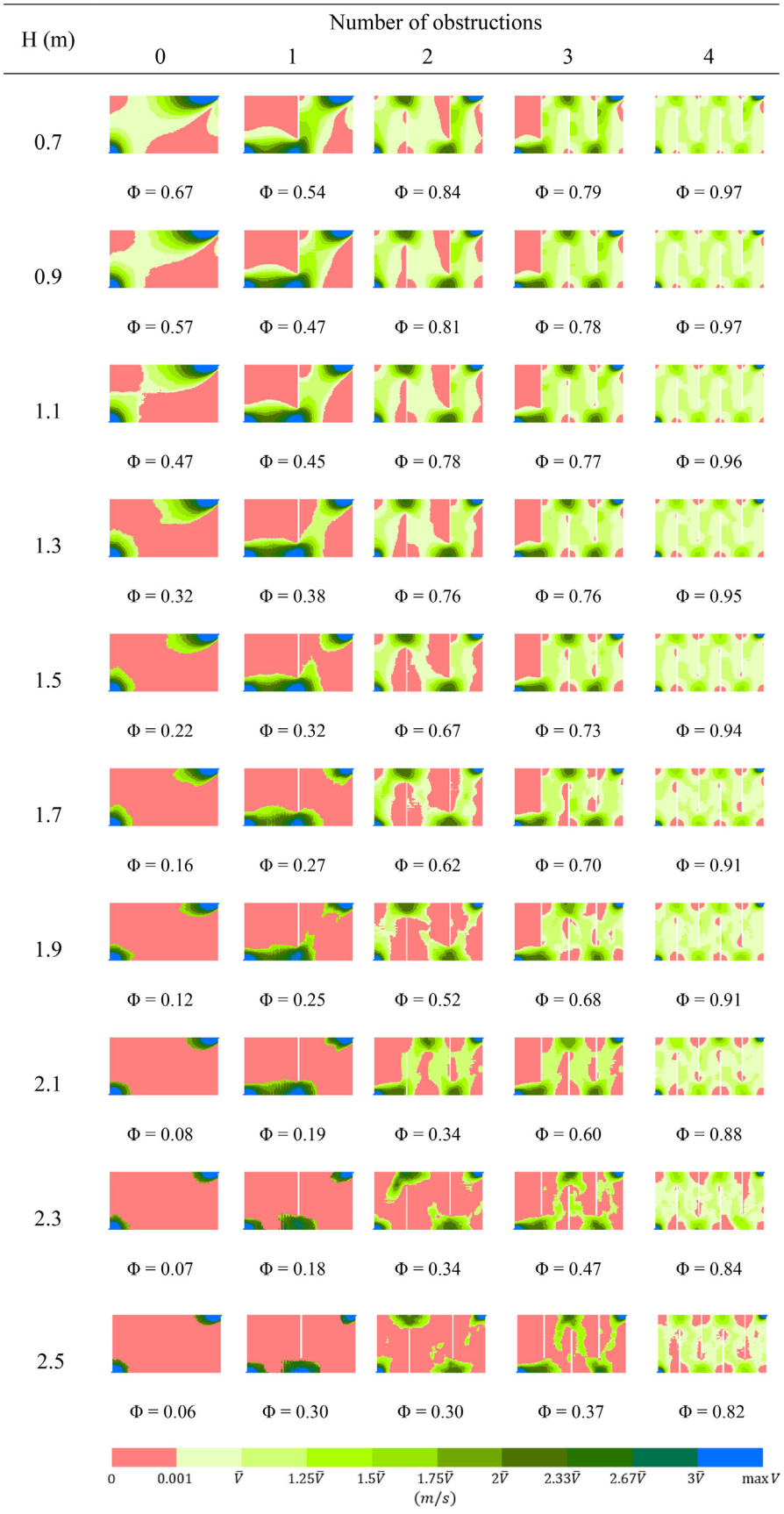

Fig. 5. Spatial variation in the flow velocity field of the fifty cases with a different number of obstructions and water depths. The red area represents low-velocity areas, while the blue area represents high-velocity areas; otherwise, the green region represents the relatively uniform flow zones. (For interpretation of the references to colour in this figure legend, the reader is referred to the web version of this article.)

(a)

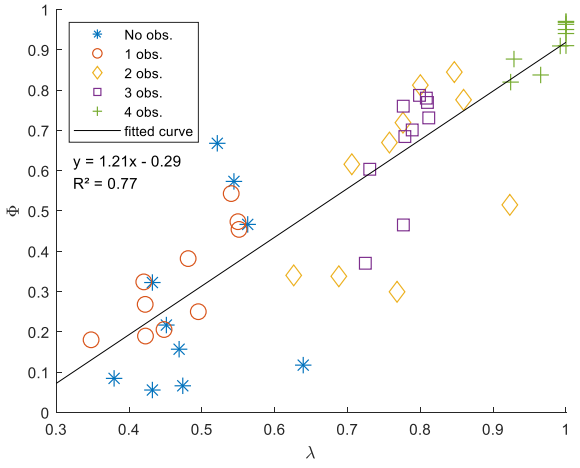

(b)

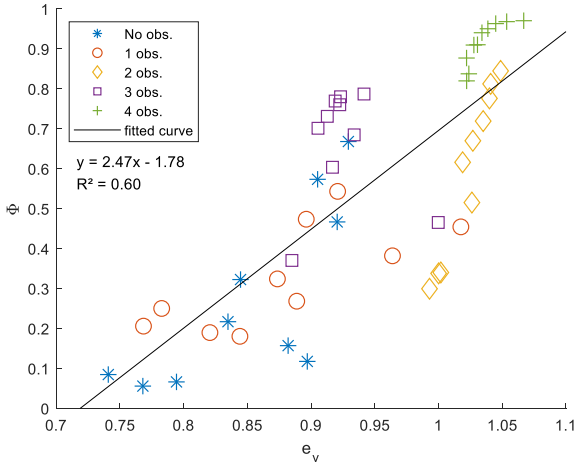

Fig. 6. The positive linear relationships between flow uniformity and hydraulic performance, including (a) hydraulic efficiency and (b) effective volume ratio.

where Φ represents the combined metric of flow uniformity, λ represents the hydraulic efficiency, and e_v represents the effective volume ratio of a wetland. The flow uniformity metric is between 0 and 1, indicating poor to excellent performance in hydraulic conditions.

The major errors of the two regressing equations are found to occur with the cases of no EOs and one EO. Further research could extend the Φ value and focus on the circulation zone. By comparing the three classes of Persson et al. (1999), we propose four classes of Φ values to represent the quality of the flow velocity distribution: (Arega, 2013) poor: $\Phi \leq 0.30$; (Bracho et al., 2006) satisfactory: $0.30 < \Phi \leq 0.60$; (Chang et al., 2016) good: $0.60 < \Phi \leq 0.80$; and (Cowan, 1956) excellent: $\Phi > 0.80$. From this classification, four EOs can construct an excellent uniform flow velocity in both shallow and deep-water wetlands and be suggested to install into the wetlands to improve the hydraulic and treatment performances. The four-class method may also be used in field surveys and flume experiments. We would have the opportunity to obtain sufficient and high-accuracy data of flow velocity with the full field investigation techniques becoming increasingly active. The method presented by this study may help evaluate the in-situ hydraulic and wetland treatment performance.

4. Conclusions

We propose an innovative method to identify dead zones and short-circuiting flow zones and establish the relationship between these combined effects and hydraulic efficiency in this study. Fifty hypothesis cases with variant water depths and obstruction numbers are quantified and analyzed by using hydrodynamic and water quality simulation models to evaluate the flow pathway, flow velocity variations, residence time, effective volume ratio, and hydraulic efficiency. The results show that the advection effect dominates contaminant transportation. The dead zone plays a significant role, while the preferential region plays a minor role in affecting flow uniformity and hydraulic performance. The dead zone area occurs when the flow velocity is lower than 1×10^{-3} m s^{-1}. With proper obstruction design, hydraulic efficiency increases by approximately 77%. The pollutant treatment efficiency was found to be negative proportional to water depths but not sensitive to altered flow uniformity. The advantage of this method is to investigate the flow field directly and yield hydraulic efficiency. Once we obtain the flow field, hydraulic performance is easily obtained, and it could be time-saving. Further study may focus on short-circuiting flow and circulation areas to achieve a more in-depth understanding of hydraulic conditions in constructed wetlands.

Declaration of Competing Interest

The authors declare that they have no known competing financial interests or personal relationships that could have appeared to influence the work reported in this paper.

Acknowledgment

The authors are grateful to the Ministry of Science and Technology, Taiwan (MOST 103-2621-M-002 -020) for funding support. The constructive suggestions from three anonymous reviewers were incorporated into the paper.

References

Arega, F., 2013. Hydrodynamic modeling and characterizing of Lagrangian flows in the West Scott Creek wetlands system, South Carolina. J. Hydro Environ. Res. 7, 50–60.
Bracho, N., Lloyd, B., Aldana, G., 2006. Optimisation of hydraulic performance to maximise faecal coliform removal in maturation ponds. Water Res. 40, 1677–1685.
Chang, T.J., Chang, Y.S., Lee, W.T., Shih, S.S., 2016. Flow uniformity and hydraulic efficiency improvement of deep-water constructed wetlands. Ecol. Eng. 92, 28–36.
Cooper, P.F., Job, G.D., Green, M.B., Shutes, R.B.E., 1996. Reed Beds and Constructed Wetlands for Wastewater Treatment. WRc Publications, Medmenham, Marlow, UK.
Cowan, W.L., 1956. Estimating hydraulic roughness coefficients. Agric. Eng. 37, 473–475.
De Oliveira, R., Pearson, H.W., Silva, J.V.N., Sousa, J.T., Leite, V.D., Lopes, W.S., 2011. Baffled primary facultative ponds with inlets and outlets set at different levels treating domestic wastewater in Northeast Brazil. Water Sci. Technol. 63, 1183.
Dierberg, F.E., Juston, J.J., DeBusk, T.A., Pietro, K., Gu, B., 2005. Relationship between hydraulic efficiency and phosphorus removal in a submerged aquatic vegetation-dominated treatment wetland. Ecol. Eng. 25, 9–23.
Donnell, B.P., Letter, J.V., McAnally, W.H., 2009. Users Guide to RMA2. Version 4.5. US Army Corps of Engineers, Waterways Experiment Station Hydraulics Laboratory.
Farjood, A., Melville, B.W., Shamseldin, A.Y., 2015. The effect of different baffles on hydraulic performance of a sediment retention pond. Ecol. Eng. 81, 228–232.
Fischer, H.B., 1967. The mechanics of dispersion in natural streams. ASCE J. Hyd. Div. 93, 187–216.
Fischer, H.B., List, E.J., Koh, R.C.Y., Imberger, J., Brooks, N.H., 1979. Mixing in Inland and Coastal Waters. Academic Press, Inc., NY, USA.
Guzman, C.B., Cohen, S., Xavier, M., Swingle, T., Qiu, W., Nepf, H., 2018. Island topographies to reduce short-circuiting in stormwater detention ponds and treatment wetlands. Ecol. Eng. 117, 182–193.
Hammer, D.A., 1989. Constructed Wetlands for Wastewater Treatment: Municipal, Industrial and Agricultural. Lewis Publishers, Chelsea, MI.
Holland, J.F., Martin, J.F., Granata, T., Bouchard, V., Quigley, M., Brown, L., 2004. Effects of wetland depth and flow rate on residence time distribution characteristics. Ecol. Eng. 23, 189–203.
Hsu, C., Hsieh, H., Yang, L., Wu, S., Chang, J., Hsiao, S., Su, H., Yeh, C., Ho, Y., Lin, H., 2011. Biodiversity of constructed wetlands for wastewater treatment. Ecol. Eng. 37, 1533–1545.
Kadlec, R.H., Knight, R.L., 1996. Treatment Wetlands. CRC Press, Lewis Publishers, Boca Raton, FL.

Kadlec, R.H., Roy, S.B., Munson, R.K., Charlton, S., Brownlie, W., 2010. Water quality performance of treatment wetlands in the Imperial Valley, California. Ecol. Eng. 36, 1093–1107.
Letter, J.V., Donnell, B.P., 2008. Users Guide for RMA4 Version 4.5. US Army, Engineer Research and Development Center Waterways Experiment Station Coastal and Hydraulics Laboratory.
Liu, J., Dong, B., Zhou, W., Qian, Z., 2020. Optimal selection of hydraulic indexes with classical test theory to compare hydraulic performance of constructed wetlands. Ecol. Eng. 143, 105687.
Musner, T., Bottacin-Busolin, A., Zaramella, M., Marion, A., 2014. A contaminant transport model for wetlands accounting for distinct residence time bimodality. J. Hydrol. 515 (16), 237–246.
Nighman, D., Harbor, J., 1997. Trap efficiency of a stormwater basin with and without baffles. In: Proc. Int. Erosion Control Assn. 28.
Persson, J., 2000. The hydraulic performance of ponds of various layouts. Urban Water 2, 243–250.
Persson, J., Wittgren, H.B., 2003. How hydrological and hydraulic conditions affect performance of treatment wetlands. Ecol. Eng. 21, 259–269.
Persson, J., Somes, N., Wong, T., 1999. Hydraulics efficiency of constructed wetlands and ponds. Water Sci. Technol. 40, 291–300.
Reed, S.C., Crites, R.W., Middlebrooks, E.J., 1995. Natural Systems for Waste Management and Treatment, Second Ed. McGraw-Hill, New York.
Sabokrouhiyeh, N., Bottacin-Busolin, A., Savickis, J., Nepf, H., Marion, A., 2017. A numerical study of the effect of wetland shape and inlet-outlet configuration on wetland performance. Ecol. Eng. 105, 170–179.
Sabokrouhiyeh, N., Bottacin-Busolin, A., Tregnaghi, M., Nepf, H., Marion, A., 2020. Variation in contaminant removal efficiency in free-water surface wetlands with heterogeneous vegetation density. Ecol. Eng. 143, 105662.
Savickis, J., Bottacin-Busolin, A., Zaramella, M., Sabokrouhiyeh, N., Marion, A., 2016. Effect of a meandering channel on wetland performance. J. Hydrol. 535, 204–210.
Shih, S.S., Kuo, P.H., Fang, W.T., LePage, B.A., 2013. A correction coefficient for pollutant removal in free water surface wetlands using first-order modeling. Ecol. Eng. 61, 200–206.
Shih, S.S., Hong, S.S., Chang, T.J., 2016. Flume experiments for optimizing the hydraulic performance of a deep-water wetland utilizing emergent vegetation and obstructions. Water 8 (6), 265.
Shih, S.S., Zeng, Y.Q., Lee, H.Y., Otte, M.L., Fang, W.T., 2017. Tracer experiments and hydraulic performance improvements in a treatment pond. Water 9 (2), 137.
Su, T.M., Yang, S.C., Shih, S.S., Lee, H.Y., 2009. Optimal design for hydraulic efficiency performance of free-water-surface constructed wetlands. Ecol. Eng. 35, 1200–1207.
Thackston, E.L., Shields, F.D., Schroeder, P.R., 1987. Residence time distributions of shallow basins. J. Environ. Eng. 113, 1319–1332.
Toet, S., Van Logtestijn, R.S.P., Schreijer, M., Kampf, R., Verhoeven, J.T.A., 2005. The functioning of a wetland system used for polishing effluent from a sewage treatment plant. Ecol. Eng. 25, 101–124.
US Environmental Protection Agency, 1988. Design Manual for Constructed Wetlands and Floating Aquatic Systems for Municipal Wastewater. US EPA Office of Research and Development, Cincinnati, OH.
USEPA, 2000. Constructed Wetlands Treatment of Municipal Wastewaters. U.S. Environmental Protection Agency, Cincinnati, OH.
Vymazal, J., 2014. Constructed wetlands for treatment of industrial wastewaters: a review. Ecol. Eng. 73, 724–751.
Wahl, M.D., Brown, L.C., Soboyejo, A.O., Martin, J., Dong, B., 2010. Quantifying the hydraulic performance of treatment wetlands using the moment index. Ecol. Eng. 36, 1691–1699.
Zedler, J.B., Kercher, S., 2005. Wetland resources: status, trends, ecosystem services, and restorability. Annu. Rev. Environ. Resour. 30, 39–74.